COMPARATIVE THERMAL BUCKLING ANALYSIS OF FUNCTIONALLY GRADED PLATE

by

**Dragan V. ČUKANOVIĆ[a*], Gordana M. BOGDANOVIĆ[b],
Aleksandar B. RADAKOVIĆ[c], Dragan I. MILOSAVLJEVIĆ[b],
Ljiljana V. VELJOVIĆ[b], and Igor M. BALAĆ[d]**

[a] Faculty of Technical Sciences, University of Pristina, Kosovska Mitrovica, Serbia
[b] Faculty of Engineering, University of Kragujevac, Kragujevac, Serbia
[c] State University of Novi Pazar, Novi Pazar, Serbia
[d] Faculty of Mechanical Engineering, University of Belgrade, Belgrade, Serbia

A thermal buckling analysis of functionally graded thick rectangular plates according to von Karman non-linear theory is presented. The material properties of the functionally graded plate, except for the Poisson's ratio, were assumed to be graded in the thickness direction, according to a power-law distribution, in terms of the volume fractions of the metal and ceramic constituents. Formulations of equilibrium and stability equations are derived using the high order shear deformation theory based on different types of shape functions. Analytical method for determination of the critical buckling temperature for uniform increase of temperature, linear and non-linear change of temperature across thickness of a plate is developed. Numerical results were obtained in MATLAB software using combinations of symbolic and numeric values. The paper presents comparative results of critical buckling temperature for different types of shape functions. The accuracy of the formulation presented is verified by comparing to results available from the literature.

Key words*: thermal buckling, von Karman non-linear theory, shape function,
higher-order shear deformation theory, power-law distribution*

Introduction

Functionally graded materials (FGM) are composite materials in which there is a continuous and a discontinuous variation of their chemical composition and/or micro-structure through defined geometric distance. Mechanical properties such as Young's modulus of elasticity, Poisson's ratio, shear modulus, as well as material thickness, are graded in recommended directions, and a gradient property can be stepwise or continuous, [1]. Delamination between layers is the biggest and the most frequently analyzed problem concerning conventional composite laminates. Most frequently used FGM is metal/ceramics, where ceramics have a good temperature resistance, while metal is superior in terms of toughness. Functionally graded materials, which contain metal and ceramic constituents, improve thermo mechanical properties between layers because of which delamination of layers should be avoided due to continuous change between properties of the constituents. By varying a percentage of volume fraction content of the two or more materials, FGM can be formed so that it achieves a desired gradient property in specific directions.

---

*Corresponding author; e-mail: dragan.cukanovic@pr.ac.rs

The thermoelastic behavior of a FG rectangular ceramic-metal plate was presented by Praveen and Reddy [2] by using a four node rectangular finite element based on the first order shear deformation theory (FSDT), including von Karman's non-linear effect. Using and expanding the adopted formulation by Praveen and Reddy, Reddy [3] studied the static analysis of the FG rectangular plates using the third order shear deformation theory (TSDT). Using the TSDT, he defined displacement field based on the finite element of the plate with the eight-degrees of freedom per node. This formulation explains the thermo mechanical coupling and von Karman's geometrical non-linearity. Woo and Meguid [4] studied non-linear deformations of thin FG plates and shells using von Karman's classical non-linear plate theory under thermo mechanical loads. The authors compared the stresses and displacements for ceramic, metal and FG plates and they concluded that displacements of the FG plate were, even with a small ceramic volume fraction, significantly smaller than displacements of the metal plate. Ma and Wang [5] researched large deformations by bending and buckling of an axisymmetrical simply supported and fixed circular FG plate using the von Karman's non-linear plate theory. The authors of the paper made an assumption that mechanical and thermal properties of FG materials vary continuously according to the power law of the volume fraction of the constituents. Lanhe [6] derived equilibrium and stability equations of a moderately thick rectangular simply supported FG plate under thermal loads using FSDT. Buckling temperature is derived for two types of thermal loading – uniform temperature increase and gradient increase through the thickness of the plate. Chi and Chung [7, 8] obtained a closed form solution of a simply supported FG rectangular moderately thick plate under transverse load using the classical plate theory and Fourier series expansion. They assumed that the elastic modulus varies in the thickness direction of the plate, depending on the variation of the volume fraction of the constituents. Poisson's ratio remains constant. Closed form analytical solution is proven by comparing to numerical results with finite element method. Chung and Che [9] analyzed a simply supported, elastic, moderately thick, rectangular FG plate under linear temperature changes in the thickness direction of the plate. They assumed that Young's modulus of elasticity and Poisson's ratio are constant throughout the plate. However, the thermal expansion coefficient varies depending on the variation of the volume fraction of the constituents, based on the power law or exponential function in the thickness direction.

Description of the problem

Functionally graded rectangular plates of $a \times b \times h$ dimensions, where the z-axis is in direction of thickness, h, are studied in this paper. Young's modulus of elasticity, thermal expansion coefficient and changes in temperature are defined according to the power law [10]:

$$E(z) = E_m + E_{cm}\left(\frac{1}{2} + \frac{z}{h}\right)^p, \quad \alpha(z) = \alpha_m + \alpha_{cm}\left(\frac{1}{2} + \frac{z}{h}\right)^p, \quad T(z) = T_m + \Delta T_{cr}\left(\frac{1}{2} + \frac{z}{h}\right)^s$$

$$E_{cm} = E_c - E_m, \quad \alpha_{cm} = \alpha_c - \alpha_m, \quad \Delta T_{cr} = T_c - T_m \tag{1}$$

respectively, where subscripts c and m refer to ceramics and metal, respectively. By using substitution $(1/2 + z/h) = \Lambda$, each of the previously mentioned laws represents a function of Λ. If the product is further defined as $E(z) \cdot \alpha(z) \cdot T(z)$, it is not difficult to conclude that for defined properties of materials and defined values of p and s (p defines the percentage of ceramic or metal volume, $0 < s < \infty$ [10]), ΔT_{cr} remains the only unknown value in the product. Analytical procedure for determining the critical buckling temperature for uniform increase of temperature, linear and non-linear change of temperature across the thickness of a plate, is developed here.

Displacement field and constitutive equations

Disadvantages of the classical lamination theory, and the first FSDT which require correctional factors, are eliminated by many authors by introducing the shear deformation shape functions (SF), tab. 1. Many of those SF are introduced in order to give the better results for specific kinds of loads and specific static or dynamical problems. It should be emphasized that the following SF are not generally applicable to all kinds of problems.

Table 1. Shear deformation SF defined by different authors

Number of shape | function	Name of authors	Shape function $f_{(z)}$
SF 1	Ambartsumain [11]	$(z/2)\left(h^2/4 - z^2/3\right)$
SF 2	Reissner and Stavsky [12]	$(5z/4)\left(1 - 4z^2/3h^2\right)$
SF 3	Stein [13]	$(h/\pi)\sin(\pi z/h)$
SF 4	Mantari, *et al.* [14]	$\sin(\pi z/h)\,e^{\cos(\pi z/h)/2} + (\pi z/2h)$
SF 5-6	Mantari *et al.* [15]	$\tan(mz) - zm\sec^2(mh/2),\ \ m = \{1/5h, \pi/2h\}$
SF 7	Karama, *et al.* [16] Aydogdu [17]	$z\exp\left[-2(z/h)^2\right],\ z\exp\left[-2(z/h)^2/\ln\alpha\right],\ \forall\alpha>0$
SF 8	Mantari, *et al.* [18]	$z \cdot 2.85^{-2(z/h)^2} + 0.028z$
SF 9	Meiche, *et al.* [19]	$\xi\left[(h/\pi)\sin(\pi z/h) - z\right],\ \ \xi = \{1, 1/\cosh(\pi/2) - 1\}$
SF 10	Soldatos [20]	$h\sinh(z/h) - z\cosh(1/2)$
SF 11	Akavci [21]	$z\sec h\left(z^2/h^2\right) - z\sec h(\pi/4)\left[1 - (\pi/2)\tanh(\pi/4)\right]$
SF 12	Akavci [21]	$(3\pi/2)h\tanh(z/h) - (3\pi/2)z\,\mathrm{sech}^2(1/2)$
SF 13	Mechab, *et al.* [22]	$\dfrac{z\cos(1/2)}{-1+\cos(1/2)} - \dfrac{h\sin(z/h)}{-1+\cos(1/2)}$

The displacement field is here taken as follows, [15]:

$$u(x,y,z,t) = u_0(x,y,t) - z\frac{\partial w}{\partial x}(x,y,t) + f(z)\theta_x$$

$$v(x,y,z,t) = v_0(x,y,t) - z\frac{\partial w}{\partial y}(x,y,t) + f(z)\theta_y \qquad (2)$$

$$w(x,y,z,t) = w_0(x,y,t)$$

where $f(z)$ is a SF. In order to define components of unit loads, it is necessary to apply the relations between displacements and strains in accordance with the von Karman's non-linear theory of elasticity [2]. Using a generalized Hooke's law, as well as the stiffness matrix [10], and taking into account the effect of the change in temperature eq. (1) and thermal expansion, which cause a strain $\alpha\Delta T$ [23], the following components of unit loads are obtained:

$$\{\mathrm{N}\} = \int_{h^-}^{h^+}\{\sigma\}\mathrm{d}z = \int_{h^-}^{h^+}[\mathrm{Q}]\{\mathrm{k}_0\}\mathrm{d}z + \int_{h^-}^{h^+}[\mathrm{Q}]\{\mathrm{k}_1\}z\mathrm{d}z + \int_{h^-}^{h^+}[\mathrm{Q}]\{\mathrm{k}_2\}f(z)\mathrm{d}z - \int_{h^-}^{h^+}[\mathrm{Q}_\mathrm{T}]\alpha(z)T(z)\mathrm{d}z$$

$$\{\mathrm{M}\} = \int_{h^-}^{h^+}\{\sigma\}z\mathrm{d}z = \int_{h^-}^{h^+}[\mathrm{Q}]\{\mathrm{k}_0\}z\mathrm{d}z + \int_{h^-}^{h^+}[\mathrm{Q}]\{\mathrm{k}_1\}z^2\mathrm{d}z + \int_{h^-}^{h^+}[\mathrm{Q}]\{\mathrm{k}_2\}zf(z)\mathrm{d}z - \int_{h^-}^{h^+}[\mathrm{Q}_\mathrm{T}]z\alpha(z)T(z)\mathrm{d}z$$

$$\{\mathrm{P}\} = \int_{h^-}^{h^+}\{\sigma\}f(z)\mathrm{d}z = \int_{h^-}^{h^+}[\mathrm{Q}]\{\mathrm{k}_0\}f(z)\mathrm{d}z + \int_{h^-}^{h^+}[\mathrm{Q}]\{\mathrm{k}_1\}zf(z)\mathrm{d}z + \int_{h^-}^{h^+}[\mathrm{Q}]\{\mathrm{k}_2\}\left[f(z)\right]^2\mathrm{d}z - \int_{h^-}^{h^+}[\mathrm{Q}_\mathrm{T}]z\alpha(z)T(z)\mathrm{d}z$$

$$\{\mathrm{R}\} = \int_{h^-}^{h^+}\{\tau\}f^{'}(z)\mathrm{d}z = \int_{h^-}^{h^+}[\mathrm{Q}_\mathrm{S}]\{\mathrm{k}_\mathrm{S}\}\left[f^{'}(z)\right]^2\mathrm{d}z$$

where

$$[\mathrm{Q}] = \begin{bmatrix} \mathrm{Q}_{11} & \mathrm{Q}_{12} & \mathrm{Q}_{16} \\ \mathrm{Q}_{12} & \mathrm{Q}_{22} & \mathrm{Q}_{26} \\ \mathrm{Q}_{16} & \mathrm{Q}_{26} & \overline{\mathrm{C}}_{66} \end{bmatrix}, \quad [\mathrm{Q}_S] = \begin{bmatrix} \mathrm{Q}_{44} & \mathrm{Q}_{45} \\ \mathrm{Q}_{45} & \mathrm{Q}_{55} \end{bmatrix}, \quad [\mathrm{Q}_T] = \begin{bmatrix} \mathrm{Q}_{11} + \mathrm{Q}_{12} \\ \mathrm{Q}_{12} + \mathrm{Q}_{22} \\ 0 \end{bmatrix}$$

$$\{\sigma\} = \left\{\sigma_{xx} \quad \sigma_{yy} \quad \sigma_{xy}\right\}^T, \quad \{\tau\} = \left\{\tau_{xz} \quad \tau_{yz}\right\}^T$$

$$\{\mathrm{N}\} = \left\{N_{xx} \quad N_{yy} \quad N_{xy}\right\}^T, \quad \{\mathrm{M}\} = \left\{M_{xx} \quad M_{yy} \quad M_{xy}\right\}^T$$

$$\{\mathrm{P}\} = \left\{P_{xx} \quad P_{yy} \quad P_{xy}\right\}^T, \quad \{\mathrm{R}\} = \left\{R_y \quad R_x\right\}^T \tag{3}$$

$$\{\mathrm{k}_0\} = \left\{\frac{\partial u_0}{\partial x} + \frac{1}{2}\left(\frac{\partial w}{\partial x}\right)^2 \quad \frac{\partial v_0}{\partial y} + \frac{1}{2}\left(\frac{\partial w}{\partial y}\right)^2 \quad \frac{\partial u_0}{\partial y} + \frac{\partial v_0}{\partial x} + \frac{\partial w}{\partial x}\frac{\partial w}{\partial y}\right\}^T$$

$$\{\mathrm{k}_1\} = \left\{-\frac{\partial^2 w_0}{\partial x^2} \quad -\frac{\partial^2 w_0}{\partial y^2} \quad -2\frac{\partial^2 w_0}{\partial x\partial y}\right\}^T$$

$$\{\mathrm{k}_2\} = \left\{\frac{\partial \theta_x}{\partial x} \quad \frac{\partial \theta_y}{\partial y} \quad \frac{\partial \theta_x}{\partial y} + \frac{\partial \theta_y}{\partial x}\right\}^T, \quad \{\mathrm{k}_\mathrm{S}\} = \left\{\theta_x \quad \theta_y\right\}^T$$

In eq. (3), by grouping the terms with the elements of constitutive matrix, it is possible to define new matrices:

$$\left(\mathrm{A}_{ij}, \mathrm{B}_{ij}, \mathrm{D}_{ij}, \mathrm{E}_{ij}, \mathrm{F}_{ij}, \mathrm{G}_{ij}\right) = \int_{h^-}^{h^+} Q_{ij}\left\{1, z, f(z), z^2, zf(z), \left[f(z)\right]^2\right\}\mathrm{d}z, \quad \text{for} \quad i, j = (1, 2, 6)$$

$$\tag{4}$$

$$H_{lr} = \int_{h^-}^{h^+} Q_{lr}\left[f^{'}(z)\right]^2\mathrm{d}z, \quad (l, r) = (4, 5)$$

In order to get an equilibrium equation, it is necessary to define the deformation energy in the following form [10]:

$$U = \int_{h^-}^{h^+} \int_A \left\{ \sigma_{xx} \left[\varepsilon_{xx} - \alpha(z)T(z) \right] + \sigma_{yy} \left[\varepsilon_{yy} - \alpha(z)T(z) \right] + \sigma_{zz}\varepsilon_{zz} + \tau_{xy}\gamma_{xy} + \tau_{xz}\gamma_{xz} + \tau_{yz}\gamma_{yz} \right\} \mathrm{d}A\mathrm{d}z \quad (5)$$

Using the principles of minimum potential energy, equilibrium equations become:

$$\delta u_0 : N_{xx,x} + N_{xy,y} = 0, \qquad \delta v_0 : N_{yy,y} + N_{xy,x} = 0$$

$$\delta w_0 : M_{xx,xx} + 2M_{xy,xy} + M_{yy,yy} + N_{xx}w_{0,xx} + 2N_{xy}w_{0,xy} + N_{yy}w_{0,yy} = 0 \qquad (6)$$

$$\delta \theta_x : P_{xx,x} + P_{xy,y} - R_x = 0, \qquad \delta \theta_y : P_{xy,x} + P_{yy,y} - R_y = 0$$

Stability equation for a thick FG plate is derived based on the equilibrium eq. (6). The stability equation of the plate under thermal load can be defined using the displacement components u_0, v_0, w_0, θ_{x0}, and θ_{y0}. Displacement components of the next stable configuration are:

$$u = u_0 + u_1, \qquad v = v_0 + v_1, \qquad w = w_0 + w_1$$

$$\theta_x = \theta_{x0} + \theta_{x1}, \quad \theta_y = \theta_{y0} + \theta_{y1} \qquad (7)$$

where u_1, v_1, w_1, θ_{x1}, and θ_{y1} are the displacement components of arbitrarily small deviation from the stable configuration. Assuming that temperature is constant in the *xy*-plane of the plate and that it is changing only in the thickness direction of the plate, the stability equation can be derived by substituting eq. (7) and eq. (3) into eq. (6). In such obtained equation, terms u_0, v_0, w_0, θ_{x0}, and θ_{y0} do not exist because they vanish due to satisfying the equilibrium condition eq. (6). Therefore, the stability equations of the functionally graded rectangular plate are:

$$\delta u_0 : N_{xx,x}^1 + N_{xy,y}^1 = 0, \qquad \delta v_0 : N_{yy,y}^1 + N_{xy,x}^1 = 0$$

$$\delta w_0 : M_{xx,xx}^1 + 2M_{xy,xy}^1 + M_{yy,yy}^1 + N_{xx}^0 w_{1,xx} + 2N_{xy}^0 w_{1,xy} + N_{yy}^0 w_{1,yy} = 0 \qquad (8)$$

$$\delta \theta_x : P_{xx,x}^1 + P_{xy,y}^1 - R_x^1 = 0, \qquad \delta \theta_y : P_{xy,x}^1 + P_{yy,y}^1 - R_y^1 = 0$$

where N_{xx}^0, N_{yy}^0, and N_{xy}^0, are the resultants of the pre-buckling forces:

$$N_{xx}^0 = N_{yy}^0 = -\int_{-h/2}^{h/2} \frac{E(z)\alpha(z)T(z)}{1-\upsilon}\mathrm{d}z, \qquad N_{xy}^0 = 0. \qquad (9)$$

Equation (8) can be solved by using the analytical and numerical methods. In order to obtain analytical solutions, assumed solution forms and boundary conditions are adopted in accordance to Navier's methods applied in [24-26]. Procedure for obtaining the results by combining the symbolic and numerical coefficient values, which occur in these kinds of problems, is implemented.

Boundary conditions along edges of the simply supported rectangular plate, according to [26], are the following:

$$v_0 = w_0 = \theta_y = N_{xx} = M_{xx} = P_{xx} = 0 \quad \text{along edges} \quad x = 0 \text{ and } x = a$$

$$u_0 = w_0 = \theta_x = N_{yy} = M_{yy} = P_{yy} = 0 \quad \text{along edges} \quad y = 0 \text{ and } y = b \qquad (10)$$

Taking into account the previously defined boundary conditions, based on [24], it is possible to assume that Navier's solution is in the following form:

$$u_1(x,y) = \sum_{m=1}^{\infty}\sum_{n=1}^{\infty} U_{mn} \cos\frac{m\pi x}{a}\sin\frac{n\pi y}{b}, \quad v_1(x,y) = \sum_{m=1}^{\infty}\sum_{n=1}^{\infty} V_{mn} \sin\frac{m\pi x}{a}\cos\frac{n\pi y}{b}$$

$$w_1(x,y) = \sum_{m=1}^{\infty}\sum_{n=1}^{\infty} W_{mn} \sin\frac{m\pi x}{a}\sin\frac{n\pi y}{b}, \quad \theta_{x1}(x,y) = \sum_{m=1}^{\infty}\sum_{n=1}^{\infty} T_{xmn} \cos\frac{m\pi x}{a}\sin\frac{n\pi y}{b} \quad (11)$$

$$\theta_{y1}(x,y) = \sum_{m=1}^{\infty}\sum_{n=1}^{\infty} T_{ymn} \sin\frac{m\pi x}{a}\cos\frac{n\pi y}{b}$$

where U_{mn}, V_{mn}, W_{mn}, T_{xmn}, T_{ymn} are arbitrary parameters, which are to be determined. Furthermore, using the Navier's solution, equilibrium equation becomes:

$$[\mathbf{L} - \Omega\mathbf{I}]\{\mathbf{U}\} = 0 \quad (12)$$

where $\mathbf{U} = \{U_{mn}\ V_{mn}\ W_{mn}\ T_{xmn}\ T_{ymn}\}^T$ and Ω is the buckling parameter. Coefficients L_{ij}, $(i, j = 1\text{-}5)$ are defined in the following way:

$$L_{11} = \alpha^2 A_{11} + \beta^2 A_{66}, \quad L_{12} = \alpha\beta(A_{12} + A_{66}), \quad L_{13} = 0, \quad L_{14} = \alpha^2 D_{11} + \beta^2 D_{66}$$

$$L_{15} = \alpha\beta(D_{12} + D_{16}), \quad L_{22} = \alpha^2 A_{66} + \beta^2 A_{22}, \quad L_{23} = 0, \quad L_{24} = \alpha\beta(D_{12} + D_{16})$$

$$L_{25} = \alpha^2 C_{66} + \beta^2 C_{22}, \quad L_{33} = \alpha^4 E_{11} + 2\alpha^2\beta^2 E_{12} + 4\alpha^2\beta^2 E_{66} + \beta^4 E_{22} \quad (13)$$

$$L_{34} = -\alpha^3 F_{11} - \alpha\beta^2 F_{12} - 2\alpha\beta^2 E_{66}, \quad L_{35} = -\alpha^2\beta F_{12} - 2\alpha^2\beta F_{66} - \beta^3 F_{22}$$

$$L_{44} = H_{44} + \alpha^2 G_{11} + \alpha^2 G_{66}, \quad L_{45} = \alpha\beta(G_{12} + G_{66}), \quad L_{55} = H_{55} + \alpha^2 G_{66} + \alpha^2 G_{22}$$

while the matrix $\mathbf{I}_{ij}$, $(i, j = 1\text{-}5)$ is defined:

$$\{\mathbf{I}\} = \begin{cases} 0, \\ \alpha^2 N_{xx}^0 + \beta^2 N_{yy}^0, \quad (i, j = 3) \end{cases} \quad (14)$$

where $\alpha = m\pi\,/\,a$, $\beta = n\pi\,/\,b$. To obtain the non-trivial solutions, it is necessary for the determinant in eq. (12) to be equal to zero:

$$|\mathbf{L} - \Omega\mathbf{I}| = 0 \quad (15)$$

Numerical results

The aim of this section is to check the accuracy and the effectiveness of the given theory in determining the critical buckling temperature of FG plates for uniform increase of temperature, linear and non-linear change temperature across thickness. In order to do that, different numerical examples are shown, and the obtained results were compared to the results available from the literature. The theory presented in this paper is verified by the examples of the square plate $a/b=1$, which was considered in [27, 28, 10]. Unlike [28], where TSDT is applied, and [27, 10] where higher order shear deformation theory (HSDT) is applied, based on just one SF, comparative analysis of all SF (tab. 1) is done here. Besides the results, which are available in the literature, this paper shows results for a/h (5 and 10) and a/b (2 and 5) ratios. Material properties, used in the numerical examples, were:

Metal (Aluminum): $E_M = 0.7\cdot10^5$ [MPa], $v = 0.3$, $\alpha_M = 23\cdot10^{-6}$ [°C^{-1}],
Ceramics (Alumina): $E_C = 3.8\cdot10^5$ [MPa], $v = 0.3$, $\alpha_C = 7.4\cdot10^{-6}$ [°C^{-1}].

Čukanović, D. V., *et al*.: Comparative Thermal Buckling Analysis of Functionally Graded Plate
THERMAL SCIENCE: Year 2017, Vol. 21, No. 6B, pp. 2957-2969

2963

Table 2. Comparison of critical buckling temperatures (ΔT_{cr}) of rectangular FGM plates under a uniform increase of temperature ($a/h = 5$, $a/h = 10$ and $m = n = 1$)

p	Source	$a/h = 5$			$a/h = 10$		
		$a/b = 1$	$a/b = 2$	$a/b = 5$	$a/b = 1$	$a/b = 2$	$a/b = 5$
0	[27]	---	---	---	1618.680	---	---
	[28]	---	---	---	1617.484	---	---
	[10]	---	---	---	1618.750	---	---
	SF 1	5583.442	10959.448	23192.800	1618.681	3747.312	12872.652
	SF 2	5583.442	10959.448	23192.800	1618.681	3747.312	12872.652
	SF 3	5585.559	10971.195	23351.112	1618.820	3748.159	12891.308
	SF 4	5621.881	11128.293	24554.451	1621.682	3764.011	13119.689
	SF 5	5583.426	10959.286	23189.151	1618.681	3747.307	12872.361
	SF 6	5587.882	10970.575	23065.303	1619.120	3749.487	12883.915
	SF 7	5590.910	10995.856	23580.381	1619.225	3750.450	12928.084
	SF 8	5591.659	10999.186	23608.379	1619.283	3750.774	12932.982
	SF 9	5591.659	10999.186	23608.379	1619.283	3750.774	12932.982
	SF 10	5583.400	10958.981	23181.701	1618.681	3747.302	12871.799
	SF 11	5591.409	10983.034	23086.289	1619.429	3751.109	12900.319
	SF 12	5584.615	10966.460	23297.570	1618.752	3747.766	12884.026
	SF 13	5583.510	10960.024	23204.664	1618.684	3747.333	12873.662
1	[27]	---	---	---	758.390	---	---
	[28]	---	---	---	757.891	---	---
	[10]	---	---	---	758.424	---	---
	SF 1	2671.531	5398.066	12201.408	758.395	1775.555	6406.862
	SF 2	2671.531	5398.066	12201.408	758.395	1775.555	6406.862
	SF 3	2672.409	5403.230	12280.777	758.450	1775.899	6415.235
	SF 4	2687.462	5472.168	12882.413	759.588	1782.344	6517.540
	SF 5	2671.524	5397.995	12199.578	758.395	1775.553	6406.732
	SF 6	2673.373	5402.958	12137.451	758.570	1776.440	6411.918
	SF 7	2674.629	5414.066	12395.630	758.611	1776.831	6431.733
	SF 8	2674.939	5415.529	12409.648	758.634	1776.963	6433.930
	SF 9	2674.939	5415.529	12409.648	758.634	1776.963	6433.930
	SF 10	2671.514	5397.861	12195.841	758.395	1775.551	6406.479
	SF 11	2674.835	5408.433	12147.980	758.692	1777.099	6419.278
	SF 12	2672.017	5401.149	12253.939	758.423	1775.740	6411.967
	SF 13	2671.559	5398.320	12207.357	758.396	1775.563	6407.316
10	[27]	---	---	---	692.690	---	---
	[28]	---	---	---	692.519	---	---
	[10]	---	---	---	692.570	---	---
	SF 1	2276.788	4205.548	7964.373	692.694	1562.032	4840.685
	SF 2	2276.788	4205.548	7964.373	692.694	1562.032	4840.685
	SF 3	2275.519	4203.601	8011.792	692.544	1561.350	4839.654
	SF 4	2290.659	4265.870	8477.768	693.799	1568.105	4929.058
	SF 5	2276.857	4205.716	7963.455	692.702	1562.066	4840.864
	SF 6	2285.447	4231.109	7961.675	693.549	1566.244	4871.915
	SF 7	2276.487	4209.521	8092.708	692.597	1561.714	4849.198
	SF 8	2276.720	4210.599	8103.084	692.615	1561.814	4850.812
	SF 9	2276.720	4210.599	8103.084	692.615	1561.814	4850.812
	SF 10	2277.006	4206.087	7961.620	692.717	1562.141	4841.265
	SF 11	2286.626	4234.654	7962.595	693.664	1566.815	4876.290
	SF 12	2275.691	4203.457	7994.618	692.570	1561.457	4838.988
	SF 13	2276.584	4205.060	7967.439	692.672	1561.928	4840.175

In the case of graded change in temperature, the temperature at the metal surface is T_M = 5 ℃. Table 2 shows the values of critical buckling temperatures of rectangular FG plates under a uniform increase of temperature. Thick and moderately thick plates were considered in ratios a/h = 5 and a/h = 10. Using the ratios, a/h = 10, a/m = 1 and p = 0, there was a good match of results for all the given SF with the results from the papers [10, 27, 28]. An insignificant deviation was noticed in the SF marked as SF4. During the analytical procedure in MATLAB, it is noticed that only SF1, SF2, SF3, SF10, SF13 could give solutions for integrals defined in eq. (4) in closed form, while in the case of other SF, a numerical integration had to be conducted. It is noticed that the difference between results obtained by different SF increases with the increase of the (a/b) ratio, and it decreases with the increase of (a/h) ratio, proving the fact that the effect of SF is inversely proportional to the plate thickness.

Figure 1(a) a shows the decrease of the difference between the obtained results with the increase of the value p, so when p > 5, the constant ratio a/h = 10 and a variable ratio (a/b), the curves merge. The SF do not have a significant effect on this behavior because the curves obtained by the use of SF3, SF10, SF12 and SF13 completely overlap, which can be clearly seen in the fig. 1(a). In fig. 1(b), it can be clearly seen that the increase of (a/h) ratio, regardless of the p value, causes the curves to asymptotically approach zero, which is in accordance with the fact that thin plates have lower resistance to temperature change.
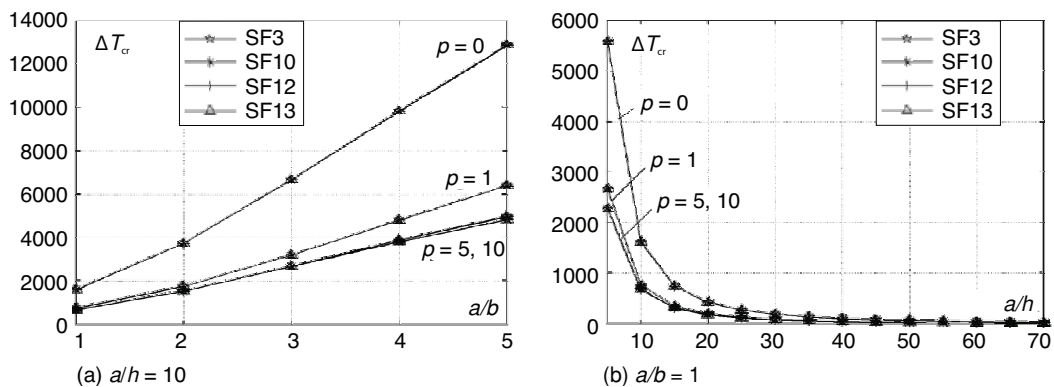
Figure 1. Effect of the aspect ratio a/b and a/h on the critical buckling temperature ΔT_{cr} under an uniform increase of temperature

Similar situation can be noticed under the linear change of temperature. All the presented SF gave the results, which match the ones from the papers [10, 27, 28]. The greatest deviation is noticed in the SF4. Table 3 shows the obtained values of the critical buckling temperature, ΔT_{cr}, as well as the matching with values given in the literature.

The curves in fig. 2(a)-2(c) are of the same nature as in the previous case. Figure 1(d) clearly shows that with the ratio values a/h = 5, a/h = 10, a/b = 1 and the increase of the value p, the curves asymptotically approach a specific value. The value of the horizontal asymptote for a rectangular plate depends mainly on the a/h ratio.

Table 4 shows numerous values of critical buckling temperatures of rectangular FG plates under a non-linear change of temperature across their thickness. There was a perfect match of the results for square plates under ratio values of a/h = 5, a/h = 10 and s = 2, s = 5 for all SF with the results given in the references [10, 27, 29]. A deviation of the results for all SF is within the permitted limits, which can be clearly seen on the diagram showing a complete overlap of curves which correspond to the different SF.

Table 3. Comparison of critical buckling temperatures (ΔT_{cr}) of rectangular FGM plates under a linear change of temperature across their thickness ($a/h = 5$, $a/h = 10$, $m = n = 1$ and $T_m = 5\ °C$)

p	Source	$a/h = 5$			$a/h = 10$		
		$a/b = 1$	$a/b = 2$	$a/b = 5$	$a/b = 1$	$a/b = 2$	$a/b = 5$
0	[27]	---	---	---	3227.360	---	---
	[28]	---	---	---	3224.968	---	---
	[10]	---	---	---	3227.510	---	---
	SF 1	11156.885	21908.895	46375.601	3227.364	7484.624	25735.303
	SF 2	11156.885	21908.895	46375.601	3227.364	7484.624	25735.303
	SF 3	11161.117	21932.391	46692.225	3227.640	7486.319	25772.617
	SF 4	11233.762	22246.586	49098.902	3233.365	7518.023	26229.378
	SF 5	11156.852	21908.572	46368.301	3227.363	7484.616	25734.721
	SF 6	11165.765	21931.151	46120.607	3228.241	7488.976	25757.830
	SF 7	11171.821	21981.711	47150.762	3228.451	7490.901	25846.167
	SF 8	11173.319	21988.372	47206.759	3228.567	7491.550	25855.963
	SF 9	11173.319	21988.372	47206.759	3228.567	7491.550	25855.963
	SF 10	11156.801	21907.961	46353.401	3227.364	7484.605	25733.597
	SF 11	11172.819	21956.069	46162.578	3228.859	7492.219	25790.637
	SF 12	11159.229	21922.920	46585.139	3227.506	7485.533	25758.051
	SF 13	11157.020	21910.049	46399.328	3227.368	7484.667	25737.324
1	[27]	---	---	---	1412.960	---	---
	[28]	---	---	---	1412.023	---	---
	[10]	---	---	---	1413.020	---	---
	SF 1	5000.989	10114.514	22873.951	1412.968	3320.615	12006.476
	SF 2	5000.989	10114.514	22873.951	1412.968	3320.615	12006.476
	SF 3	5002.635	10124.198	23022.805	1413.071	3321.261	12022.180
	SF 4	5030.867	10253.490	24151.154	1415.205	3333.348	12214.049
	SF 5	5000.976	10114.380	22870.518	1412.967	3320.612	12006.231
	SF 6	5004.443	10123.687	22754.003	1413.295	3322.275	12015.958
	SF 7	5006.798	10144.520	23238.207	1413.373	3323.009	12053.121
	SF 8	5007.381	10147.264	23264.499	1413.416	3323.257	12057.241
	SF 9	5007.381	10147.264	23264.499	1413.416	3323.257	12057.241
	SF 10	5000.956	10114.129	22863.511	1412.968	3320.608	12005.758
	SF 11	5007.186	10133.956	22773.750	1413.525	3323.512	12029.762
	SF 12	5001.901	10120.295	22972.472	1413.021	3320.962	12016.051
	SF 13	5001.042	10114.989	22885.109	1412.969	3320.631	12007.327
10	[27]	---	---	---	1218.630	---	---
	[28]	---	---	---	1218.328	---	---
	[10]	---	---	---	1218.420	---	---
	SF 1	4025.755	7443.641	14104.519	1218.639	2759.160	8569.143
	SF 2	4025.755	7443.641	14104.519	1218.639	2759.160	8569.143
	SF 3	4023.504	7440.189	14188.549	1218.372	2757.952	8567.316
	SF 4	4050.334	7550.535	15014.289	1220.596	2769.923	8725.746
	SF 5	4025.876	7443.938	14102.892	1218.652	2759.221	8569.461
	SF 6	4041.099	7488.936	14099.738	1220.154	2766.624	8624.486
	SF 7	4025.220	7450.681	14331.938	1218.467	2758.597	8584.229
	SF 8	4025.632	7452.592	14350.324	1218.498	2758.774	8587.089
	SF 9	4025.632	7452.592	14350.324	1218.498	2758.774	8587.089
	SF 10	4026.140	7444.595	14099.641	1218.680	2759.354	8570.171
	SF 11	4043.188	7495.218	14101.369	1220.358	2767.635	8632.239
	SF 12	4023.810	7439.935	14158.116	1218.418	2758.142	8566.137
	SF 13	4025.392	7442.776	14109.953	1218.600	2758.976	8568.240

2966

Čukanović, D. V., *et al.*: Comparative Thermal Buckling Analysis of Functionally Graded Plate
THERMAL SCIENCE: Year 2017, Vol. 21, No. 6B, pp. 2957-2969

Table 4. Comparision of critical buckling temperatures (ΔT_{cr}) of rectangular FGM plates under a non-linear change of temperature across their thickness ($a/h = 5$, $a/h = 10$, $m = n = 1$ and $T_m = 5$ °C)

| p | Source | $a/h = 5$ | | | | $a/h = 10$ | | | |
| | | $a/b = 1$ | | $a/b = 5$ | | $a/b = 1$ | | $a/b = 5$ | |
		$s = 2$	$s = 5$	$s = 2$	$s = 5$	$s = 2$	$s = 5$	$s = 2$	$s = 5$
0	[27]	16730.0	33470.0	---	---	4840.0	9680.0	---	---
	[29]	16741.6	33483.3	---	---	4841.4	9682.9	---	---
	[10]	16738.8	33477.7	---	---	4841.2	9682.5	---	---
	SF 1	16735.3	33470.6	69563.4	139126.8	4841.0	9682.0	38602.9	77205.9
	SF 2	16735.3	33470.6	69563.4	139126.8	4841.0	9682.0	38602.9	77205.9
	SF 3	16741.6	33483.3	70038.3	140076.7	4841.4	9682.9	38658.9	77317.8
	SF 4	16850.6	33701.2	73648.3	147296.7	4850.0	9700.0	39344.0	78688.1
	SF 5	16735.2	33470.5	69552.4	139104.9	4841.0	9682.0	38602.0	77204.1
	SF 6	16748.6	33497.2	69180.9	138361.8	4842.3	9684.7	38636.7	77273.4
	SF 7	16757.7	33515.4	70726.1	141452.3	4842.6	9685.3	38769.2	77538.5
	SF 8	16759.9	33519.9	70810.1	141620.3	4842.8	9685.7	38783.9	77567.8
	SF 9	16759.9	33519.9	70810.1	141620.3	4842.8	9685.7	38783.9	77567.8
	SF 10	16735.2	33470.4	69530.1	139060.2	4841.0	9682.0	38600.4	77200.7
	SF 11	16759.2	33518.4	69243.8	138487.7	4843.2	9686.5	38685.9	77371.9
	SF 12	16738.8	33477.6	69877.7	139755.4	4841.2	9682.5	38637.0	77274.1
	SF 13	16735.5	33471.0	69598.9	139198.0	4841.0	9682.1	38605.9	77211.9
1	[27]	7450.0	15280.0	---	---	2100.0	4310.0	---	---
	[29]	7458.6	15287.8	---	---	2106.8	4318.2	---	---
	[10]	7457.5	15285.6	---	---	2106.7	4318.1	---	---
	SF 1	7456.1	15282.8	34103.5	69901.7	2106.6	4317.9	17900.8	36691.1
	SF 2	7456.1	15282.8	34103.5	69901.7	2106.6	4317.9	17900.8	36691.1
	SF 3	7458.5	15287.8	34325.5	70356.5	2106.7	4318.2	17924.2	36739.1
	SF 4	7500.6	15374.1	36007.7	73804.7	2109.9	4324.7	18210.3	37325.5
	SF 5	7456.1	15282.7	34098.4	69891.2	2106.6	4317.9	17900.4	36690.4
	SF 6	7461.2	15293.3	33924.7	69535.1	2107.1	4318.9	17914.9	36720.1
	SF 7	7464.8	15300.5	34646.6	71014.8	2107.2	4319.1	17970.3	36833.7
	SF 8	7465.6	15302.3	34685.8	71095.1	2107.3	4319.3	17976.5	36846.3
	SF 9	7465.6	15302.3	34685.8	71095.1	2107.3	4319.3	17976.5	36846.3
	SF 10	7456.0	15282.7	34088.0	69869.7	2106.6	4317.9	17899.7	36689.0
	SF 11	7465.3	15301.7	33954.1	69595.4	2107.4	4319.6	17935.5	36762.3
	SF 12	7457.5	15285.6	34250.4	70202.7	2106.7	4318.1	17915.1	36720.4
	SF 13	7456.2	15282.9	34120.2	69935.8	2106.6	4317.9	17902.1	36693.7
10	[27]	5540.0	9530.0	---	---	1670.0	2880.0	---	---
	[29]	5536.9	9525.5	---	---	1676.6	2884.4	---	---
	[10]	5537.3	9526.2	---	---	1676.7	2884.5	---	---
	SF 1	5540.0	9530.8	19409.8	33392.1	1677.0	2885.0	11792.3	20287.2
	SF 2	5540.0	9530.8	19409.8	33392.1	1677.0	2885.0	11792.3	20287.2
	SF 3	5536.9	9525.5	19525.5	33591.0	1676.6	2884.4	11789.8	20282.9
	SF 4	5573.8	9589.0	20661.8	35545.9	1679.7	2889.7	12007.9	20658.0
	SF 5	5540.1	9531.1	19407.6	33388.2	1677.0	2885.1	11792.8	20287.9
	SF 6	5561.1	9567.2	19403.2	33380.7	1679.1	2888.6	11868.5	20418.2
	SF 7	5539.2	9529.6	19722.8	33930.5	1676.7	2884.6	11813.1	20322.9
	SF 8	5539.8	9530.5	19748.1	33974.0	1676.8	2884.7	11817.0	20329.7
	SF 9	5539.8	9530.5	19748.1	33974.0	1676.8	2884.7	11817.0	20329.7
	SF 10	5540.5	9531.7	19403.1	33380.5	1677.0	2885.1	11793.8	20289.6
	SF 11	5564.0	9572.1	19405.5	33384.6	1679.3	2889.1	11879.2	20436.6
	SF 12	5537.3	9526.2	19483.6	33519.0	1676.7	2884.5	11788.2	20280.1
	SF 13	5539.5	9530.0	19417.3	33404.9	1676.9	2885.0	11791.1	20285.1
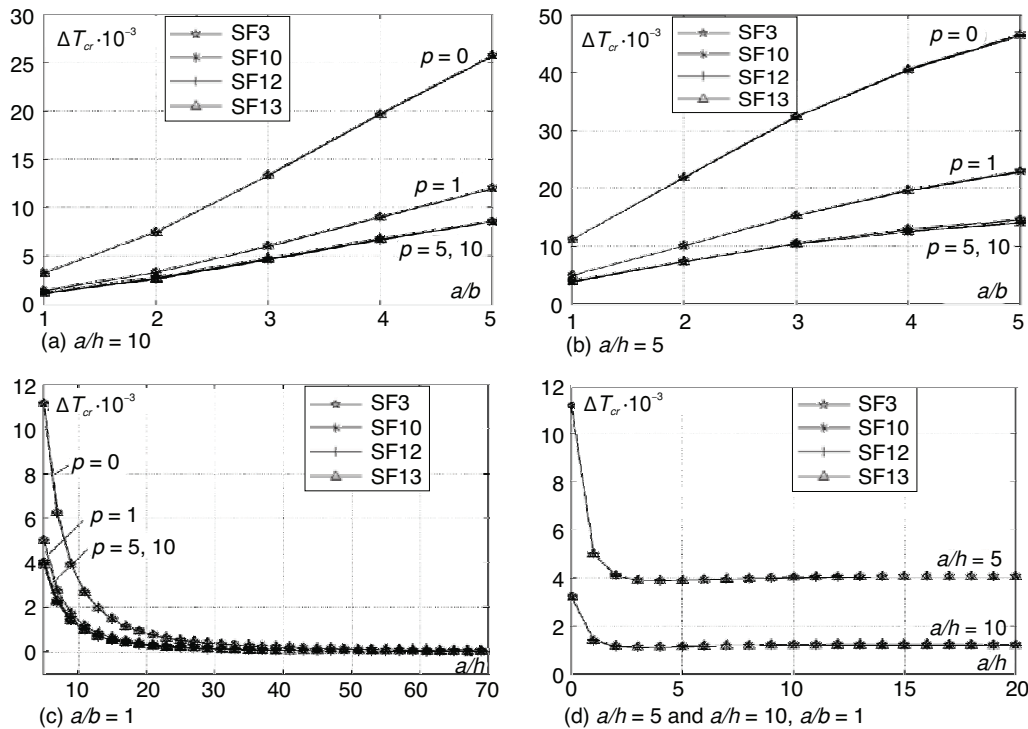
Figure 2. Effect of the aspect ratio *a/b* and *a/h* on the critical buckling temperature ΔT_{cr} under a linear change of temperature

Figure 3(c) shows that the increase of non-linearity of temperature change causes the fastest increase of ΔT_{cr} for the value $p = 0$. For larger p values, curves of the temperature change increase somewhat more slowly, but comparing to the previous cases, there is no complete matching of curves when $p = 5$ or $p = 10$. For the value $s > 6$, these curves start to go in the different directions and their separation is clearly seen.
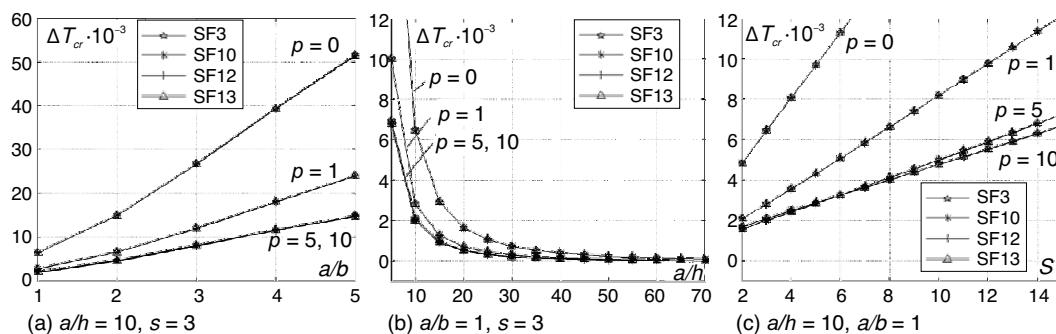
Figure 3. Effect of the aspect ratio *a/b*, *a/h* and parameter *s* on the critical buckling temperature ΔT_{cr} under a non-linear change of temperature

Conclusion

Based on the presented results, it can be concluded that SF given in tab. 1 are accept-able for the thermo mechanical analysis of functionally graded plates. The results obtained

through the developed analytical procedure matched the results given in the literature. Taking into account the fact that SF have a significantly larger effect on thick and moderately thick plates, results are limited to ratios $a/h = 5$ and $a/h = 10$. This paper proves that the volume fraction of metal//ceramic constituents and the shape of the plate (a/b ratio), have a significantly larger effect on the temperature resistance than the chosen deformation theory. It is also shown that the biggest deviations occur when the value of the parameter p is low, while the increase of the value p causes the differences between the critical temperatures to be reduced or completely vanish. Separation of the curves, which correspond to the greater values of the parameter p, occurs with the increase of non-linearity of a temperature change, namely with the increase of the s parameter.

Nomenclature

a, b, h – plate length, width, thickness, [m]
E_c, E_m – elasticity modulus of ceramics, metals, [Pa]
$f(z)$ – shape function, [–]
$\{k_0\}$ – membrane strain components, [–]
$\{k_1\}$ – strain components due to bending, [–]
$\{k_2\}$ – strain components due to plane shear, [–]
$\{k_s\}$ – strain components due to transversal shear, [–]
$\{N\}$ – force resultant per unit lenght, [Nm^{-1}]
$\{M\}$ – moment resultant per unit lenght, [N]
$\{P\}, \{R\}$ – high order moment resultants per unit lenght, [Nm]
$\{Q\}$ – constitutive matrix, [Pa]
T_c, T_m – temperature of ceramic, metal, [ºC]
ΔT_{cr} – critical buckling temperature, [ºC]
u, v, w – displacement components at a general point of plate, [m]
u_0, v_0, w_0 – displacement components at mid-plane of plate, [m]

Greek symbols

α_c, α_m – coefficient of thermal expansion of ceramics, metals, [ºC^{-1}]
θ_x, θ_y – rotation of transversal normal due to transverse shear, [–]
$\{\sigma\}$ – plane stresses components, [Pa]
$\{\tau\}$ – transversal shear stresses components, [Pa]
$\{\Omega\}$ – buckling parametar, [–]

Acronyms

FGM – functionally graded material
CPT – classical plate theory
FSDT – first order shear deformation theory
TSDT – third order shear deformation theory
HSDT – high order shear deformation theory
FEM – finite element method
MATLAB – Matrix laboratory

Superscripts

p – volume fraction index, [–]
s – degree of power law function, [–]

References

[1] Markovic, S., Sinteza i karakterizacija BaTi$_{1-x}$Sn$_x$O$_3$ prahova i viseslojnih keramickih materijala (Synthesis and Characterization of BaTi$_{1-x}$Sn$_x$O$_3$ Powders and Multilayer Ceramic Materials – in Serbian), Ph. D. thesis, University of Belgrade, Belgrade, Serbia, 2008
[2] Praveen, G. N., Reddy, J. N., Nonlinear Transient Thermoelastic Analysis of Functionlly Graded Ceramic–Metal Plates, *International Journal of Solids and Structures, 35* (1998), 33, pp. 4457-4476
[3] Reddy, J. N., Analysis of Functionally Graded Plates, *International Journal for Numerical Methods in Engineering, 47* (2000), 1-3, pp. 663-684
[4] Woo, J., Meguid, S. A., Nonlinear Analysis of Functionally Graded Plates and Shallow Shells, *International Journal of Solids and Structures, 38* (2001), 42-43, pp. 7409-7421
[5] Ma, L. S., Wang, T. J., Nonlinear Bending and Post-Buckling of a Functionally Graded Circular Plate under Mechanical and Thermal Loadings, *International Journal of Solids and Structures, 40* (2003), 13-14, pp. 3311-3330
[6] Lanhe, W., Thermal Buckling of a Simply Supported Moderately Thick Rectangular FGM Plate, *Composite Structures, 64*, (2004) 2, pp. 211-218
[7] Chi, S.-H., Chung, Y.-L., Mechanical Behavior of Functionally Graded Material Plates under Transverse Load-Part I: Analysis, *International Journal of Solids and Structures, 43* (2006), 13, pp. 3657-3674
[8] Chi, S.-H., Chung, Y.-L., Mechanical Behavior of Functionally Graded Material Plates under Transverse Load-Part II: Numerical Results, *International Journal of Solids and Structures, 43* (2006), 13, pp. 3675-3691

Čukanović, D. V., *et al.*: Comparative Thermal Buckling Analysis of Functionally Graded Plate
THERMAL SCIENCE: Year 2017, Vol. 21, No. 6B, pp. 2957-2969

2969

[9] Chung, Y.-L., Che, W.-T., The flexibility of Functionally Graded Material Plates Subjected to Uniform Loads, *Journal of Mechanics of Materials and Structures, 2* (2007), 1, pp. 63-86

[10] Akavci, S. S., Thermal Buckling Analysis of Functionally Graded Plates on an Elastic Foundation According to a Hyperbolic Shear Deformation Theory, *Mechanics of Composite Materials, 50* (2014), 2, pp. 197-212

[11] Ambartsumyan, S. A., On the Theory of Anisotropic Shells and Plates, *Proceedings*, Non-Homogeniety in Elasticity and Plasticity, IUTAM, Symposium, (Ed. W. Olszak), Warsaw, 1958

[12] Reissner, E., Stavsky, Y., Bending and Stretching of Certain Types of Heterogeneous Aeolotropic Elastic Plates, *ASME Journal of Applied Mechanics, 28* (1961), 3, pp. 402-408

[13] Stein, M., Nonlinear Theory for Plates and Shells Including the Effects of Transverse Shearing, *AIAA Journals, 24* (1986), 9, pp. 1537-1544

[14] Mantari, J. L., *et al.*, Bending and Free Vibration Analysis of Isotropic and Multilayered Plates and Shells by Using a New Accurate Higherorder Shear Deformation Theory, *Composites Part B: Engineering, 43* (2012), 8, pp. 3348-3360

[15] Mantari, J. L., *et al.*, A New Trigonometric Shear Deformation Theory for Isotropic, Laminated Composite and Sandwich Plates, *International Journal of Solids and Structures, 49* (2012), 1, pp. 43-53

[16] Karama, M., *et al.*, Mechanical Behaviour of Laminated Composite Beam by the New Multi-Layered Laminated Composite Structures Model with Transverse Shear Stress Continuity, *International Journal of Solids and Structures, 40* (2003), 6, pp. 1525-1546

[17] Aydogdu, M., A New Shear Deformation Theory for Laminated Composite Plates, *Composite Structures, 89* (2009), 1, pp. 94-101

[18] Mantari, J. L., *et al.*, A New Tangential-Exponential Higher Order Shear Deformation Theory for Advanced Composite Plates, *Composites Part B: Engineering, 60* (2014), Apr., pp. 319-328

[19] Meiche, N. E. *et al.*, A New Hyperbolic Shear Deformation Theory for Buckling and Vibration of Functionally Graded Sandwich Plate, *International Journal of Mechanical Sciences, 53* (2011), 4, pp. 237-247

[20] Soldatos, K., A Transverse Shear Deformation Theory for Homogeneous Monoclinic Plates, *Acta Mechanica, 94* (1992), 3, pp. 195-220

[21] Akavci, S. S., Two New Hyperbolic Shear Displacement Models for Orthotropic Laminated Composite Plates, *Mechanics of Composite Materials, 46* (2010), 2, pp. 215-226

[22] Mechab, B., *et al.*, Analysis of Thick Orthotropic Laminated Composite Plates Based on Higher Order Shear Deformation Theory by the New Function Under Thermo-Mechanical Loading, *Composites Part B: Engineering, 43* (2012), 3, pp. 1453-1458

[23] Milosavljević D. I., *at al.*, Failure Criteria of Fibre Reinforced Composites in Homogenous Temperature Field, *Thermal Science, 14* (2010), Suppl., pp. S285-S297

[24] Mantari, J. L., *et al.*, Bending Response of Functionally Graded Plates by Using a new Higher Order Shear Deformation Theory, *Composite Structures, 94* (2012), 2, pp. 714-723

[25] Grover, N., *et al.*, Flexural Behavior of General Laminated Composite and Sandwich Plates Using a Secant Function Based Shear Deformation Theory, *Latin American Journal of Solids and Structures, 11* (2014), 7, pp. 1275-1297

[26] Reddy. J. N., *Mechanics of Laminated Composite Plates and Shells: Theory and Analysis*, CRC Press, Boca Raton, Fla., USA, 2004

[27] Bouiadjra, M. B., *et al.*, Thermal Buckling of Functionally Graded Plates According to a Four-Variable Refined Plate Theory, *Journal of Thermal Stresses, 35* (2012), 8, pp. 677-694

[28] Javaheri, R., Eslami, M. R., Thermal Buckling of Functionally Graded Plates Based on a Higher Order Theory, *Journal of Thermal Stresses, 25* (2002), 7, pp. 603-625

[29] Zenkour, A. M., Mashat, D. S., Thermal Buckling Analysis of Ceramic-Metal Functionally Graded Plates, *Natural Science, 2* (2010), 9, pp. 968-978